



Published in final edited form as:

Proc SPIE. 2010 March 1; 7577: 75770K. doi:10.1117/12.840412.

Metal Enhanced Intrinsic Fluorescence of Proteins and Label-Free Bioassays

Krishanu Ray^{*}, Henryk Szmecinski, Mustafa H. Chowdhury, and Joseph R. Lakowicz
Center for Fluorescence Spectroscopy, University of Maryland at Baltimore, Department of Biochemistry and Molecular Biology, 725 West Lombard Street, Baltimore, MD 21201, USA

Abstract

Most of the applications of fluorescence require the use of labeled drugs and labeled biomolecules. Due to the need of labeling biomolecules with extrinsic fluorophores, there is a rapidly growing interest in methods which provide label-free detection (LFD). Proteins are highly fluorescent, which is due primarily to tryptophan residues. However, since most proteins contain tryptophan, this emission is not specific for proteins of interest in a biological sample. This is one of the reasons of not utilizing intrinsic tryptophan emission from proteins to detect specific proteins. Here, we present the intrinsic fluorescence for several proteins bound to the silver or aluminum metal nanostructured surfaces. We demonstrate the metal enhanced fluorescence (MEF) of proteins with different numbers of tryptophan residues. Large increases in fluorescence intensity and decreases in lifetime provide the means of direct detection of bound protein without separation from the unbound. We present specific detection of individual types of proteins and measure the binding kinetics of proteins such as IgG and streptavidin. Additionally, specific detection of IgG and streptavidin has been accomplished in the presence of large concentrations of other proteins in sample solutions. These results will allow design of surface-based assays with biorecognitive layer that specifically bind the protein of interest and thus enhance its intrinsic fluorescence. The present study demonstrates the occurrence of MEF in the UV region and thus opens new possibilities to study tryptophan-containing proteins without labeling with longer wavelength fluorophores and provides an approach to label-free detection of biomolecules.

Keywords

plasmonics; metal enhanced fluorescence; aluminum nanostructures; label free detection

1. INTRODUCTION

Fluorescence detection is a central technology in biological research and medical practice. Fluorescence detection presently is a central technology in the biosciences. The applications of fluorescence include cell imaging, medical diagnostics and biophysical research. Another growing use of fluorescence is for measurements of a large number of samples as occur on DNA arrays, protein arrays and high throughput screening (HTS). HTS typically includes testing of a large number of small molecules for biological activity, most often drug-receptor interactions. Almost all the applications of fluorescence require the use of labeled drugs and labeled biomolecules, which becomes increasingly inconvenient as the number of compounds to be tested have increased.

© 2010 SPIE

*krishanu@cfs.biomet.umaryland.edu; phone 1 410 706 7500; fax 1 410 706 8408; <http://cfs.umbi.umd.edu>.

The need for labeling with fluorophore has resulted in a dramatic increase in methods which do not require labeling, label-free detection. A variety of approaches have been used for label-free detection. Perhaps the most widely used and known is surface plasmon resonance (SPR). The method of SPR depends on the resonance absorption of light by a gold film illuminated through a glass prism [1–2]. The sample is located on the distal side of the gold film which is in contact with the metal. A decrease in reflection is observed at a certain angle of incidence, which is due to the creation of plasmon on the sample side of the gold film. The angle of minimum reflection is called the surface plasmon angle θ_{sp} . The angle is sensitive to the refractive index of the sample immediately above the gold film. Binding of biomolecules to the surface results in small changes in the refractive index, which in turn result in a measurable changes in the surface plasmon angle. While SPR is a sensitive method measuring the changes in θ_{sp} , requires rather precise optics and careful control of the temperature and correction for changes in refractive index upon addition of the solvents containing the compound to be detected [3]. As a result there is a growing interest in method to increase the sensitivity of SPR. These methods typically use metal nanostructures such as colloids [4–5] or periodic structures [6–7]. Because of its importance a number of other approaches are being developed for label-free detection [8–9]. These methods include interferometry [10], infrared absorption [11], oblique-incidence reflectivity [12], and photonic crystals [13] to name a few. Most methods for label-free detection share a similar property with SPR, which is a dependence on the change in biomolecular mass at the interface between sample and sensing surface and use of the resulting changes in measurements of the refractive index at the interface.

We have demonstrated the fluorescence of visible and NIR fluorophores can be increased by proximity to metal particles [14]. We observed a variety of favorable effects due to metal particles, such as increased fluorescence intensities, decrease lifetime, increased photostability and increased distances for fluorescence resonance energy transfer (FRET). We refer to these favorable effects as metal-enhanced fluorescence (MEF). MEF is increasingly finding applications in various fields including chemistry and biology. MEF is a complex phenomenon. Knowing more about MEF at the single molecule level will help implementing this phenomenon in versatile applications.

Here, we present the intrinsic fluorescence for several proteins bound to the metal nanostructured surfaces. Large increases in fluorescence intensity and decreases in lifetime provide the means of direct detection of bound protein without separation from the unbound. We present specific detection of individual types of proteins and measure the binding kinetics of proteins such as IgG and streptavidin. These results will allow design of surface-based assays with biorecognitive layer that specifically bind the protein of interest and thus enhance its intrinsic fluorescence.

2. EXPERIMENTAL SECTION

Aluminum slugs and silicon monoxide, were purchased from Sigma-Aldrich and used as received. 10 nm thick aluminum was deposited on quartz slides using an Edwards Auto 306 Vacuum Evaporation chamber under high vacuum ($<5 \times 10^{-7}$ Torr). In each case, the metal deposition step was followed by the deposition of 5 nm of silica via evaporation without breaking vacuum. This step served to protect the metal surface as well as it adds a spacer layer between the metal surface and fluorophore. The deposition rate was adjusted by the filament current and the thickness of film was measured with a quartz crystal microbalance. A portion of the sample was cut and mounted on an Al stub with conductive tape, and then observed in an Hitachi SU-70 scanning electron microscope (SEM) directly, i.e., without any further treatment of the sample. Due to the nonconductive substrate (SiO_2), ultra-low voltage was employed for high resolution shallow surface observation and imaging using beam deceleration technology. Samples were surveyed at low magnifications to see the general features and the

homogeneity. Representative areas were selected for higher magnification investigation. An Oxford Energy-dispersive X-ray spectrometer (EDS) with silicon drift detector (SSD) attached on the SEM was also used for micro-chemical analysis.

Bovine serum albumin (BSA), biotinylated bovine serum albumin (BSA-bt), streptavidin (SA), goat and rabbit immunoglobulins (IgG), were purchased from Sigma Aldrich (St. Louis, MO). Distilled water (with a resistivity of 18.2 MΩ-cm) purified using Millipore Milli-Q gradient system was used for sample preparation. We have directly deposited proteins on the aluminum nanostructured surfaces and bare quartz substrates, by non-covalent electrostatic immobilization. The biochemical procedures of protein immobilization, incubation for binding and measurements were performed in phosphate buffer saline (PBS) at pH 7.4 and room temperature.

Fluorescence spectra of probes on solid substrates were recorded using a Varian Cary Eclipse Fluorescence Spectrophotometer. Both the steady-state and time-domain lifetime measurements were carried out using front face illumination. Time-domain lifetime measurements were obtained on a PicoQuant lifetime fluorescence spectrophotometer (Fluotime 100). The excitation source was a pulsed laser diode (PicoQuant PDL800-B) with a 20 MHz repetition rate. The Instrument Response Function (IRF) is about 60 ps. Intensity decays were measured through bandpass interference filters. Emission lifetimes were measured with vertically polarized excitation. Magic angle observation was used in the emission path for the time-domain measurements. This optical configuration reduced scattered light of the excitation wavelength without significant distortion of the spectra or lifetimes.

The fluorescence intensity decays were analyzed in terms of the multi-exponential model as the sum of individual single exponential decays [15]:

$$I(t) = \sum_{i=1}^n \alpha_i \exp(-t/\tau_i) \quad (1)$$

In this expression τ_i are the decay times and α_i are the amplitudes and $\sum_i \alpha_i = 1.0$. The fractional contribution of each component to the steady-state intensity is described by:

$$f_i = \frac{\alpha_i \tau_i}{\sum_j \alpha_j \tau_j} \quad (2)$$

The average lifetime is represented by:

$$\bar{\tau} = \sum_i f_i \tau_i \quad (3)$$

The values of α_i and τ_i were determined using the PicoQuant Symphotime software with nonlinear least squares fitting. The goodness-of-fit was determined by the χ^2 value.

3. RESULTS AND DISCUSSION

Figure 1 shows the scanning electron microscope (SEM) image of the aluminum nanostructure substrates that have been used for this study. The deposition of 10 nm of aluminum (determined

with the crystal microbalance) resulted in highly packed heterogeneous nanostructures of 50–100 nm size.

First we studied immunoglobulins, which contain six tryptophan residues. Quartz and aluminum nanostructured substrates were incubated in buffer solution of IgG (10 $\mu\text{g/ml}$) for 2 hour at room temperature in a humid chamber. Slides were then rinsed with buffer, washing solution (0.05% Tween 20), and placed in buffer for measurements. Figure 2 shows that goat IgG bound on aluminum nanostructured substrate gives an emission intensity enhancement of approximately 5 – 6 fold when compared to the quartz. The intensity decays of tryptophan residues in IgG are faster on aluminum substrate compared to that on bare quartz (Figure 3). The average emission lifetime of IgG was decreased by approximately 6-fold on aluminum. The shorter lifetime and increased intensity on the aluminum nanostructures indicate that there is an interaction between excited tryptophan residues and plasmons created due to the presence of aluminum nanoparticles/nanostructures.

The most important aspect of using intrinsic fluorescence of proteins would be ability to detect the analyte in the presence of bulk concentrations of other biomolecules in the sample. Usually, the expected concentrations are high; e.g. human serum or blood is dominated with human serum albumin with about a 1 mg/ml concentration. The high concentration of biomolecules in the sample may cause that the signal from bulk proteins can be very high compared to that of specifically bound analytes. Since the effect of plasmons on fluorescence is given by near-field effect, one can design a MEF-based assay where the signal from bulk proteins can be significantly reduced. We have performed experiments where we used high concentration of BSA (bulk protein) and temporally studied binding of streptavidin to activated surface coated with biotinylated BSA. In Figure 4 are shown schematics of our approach to MEF-based label-free sensing with comparison to non-MEF (bare quartz) and control non-sensing substrate.

Figure 5 illustrates our results of binding of streptavidin to the sensing surface. After contacting sensing surface with sample that contained of 1560 nM of BSA and 157 nM SA we observed substantial increase in intensity over the time for MEF sensing surface. Despite large concentration of bulk proteins (both BSA and SA) the bound form of SA generated an easy measurable intensity signal. It should be noted that generated additional signal is on top of that MEF signal from immobilized capture BSA-Bt layer. The non-binding layer with BSA (b) resulted in small increase in signal which is due to non specific binding of SA. The control configuration on bare quartz does not show a reasonable change in intensity. This is because the bound SA does not generate more signal from that unbound, thus there is no differentiation between bound and unbound. These studies clearly indicate that MEF-based approach allow for direct detection of bound analyte in the presence of bulk sample.

In general, the detectability of a fluorophore is determined by two factors: the extent of background emission from the sample and the photostability of the fluorophore. Accordingly, we have made a comparison between the photostability of the BSA-biotin-streptavidin on quartz and aluminum substrates (Figure 6). It must be noted that in Figure 6, the incident excitation power on the aluminum nanostructured films have been attenuated to give the similar initial emission intensity on the aluminum (at $time = 0\text{ min}$) as observed on the quartz substrate. It is apparent from Figure 6 that BSA-biotin-streptavidin are more photostable on the 10 nm thick particulate aluminum substrate than on the quartz substrate.

4. CONCLUSION

We have observed aluminum nanostructure enhanced intrinsic fluorescence from proteins containing different number of tryptophan residues. Our measurements suggested the occurrence of MEF with tryptophan-containing proteins in the ultraviolet spectral region. Our

preliminary results suggest that aluminum nanostructures can potentially be employed in the ultra-violet region in various plasmon-controlled fluorescence applications to enhance the intrinsic emission of biomolecules and increase biomolecule detectability, thereby negating the need for externally tagging biomolecules and overcoming the problems associated with it.

Acknowledgments

This work was supported by the National Institutes of Health (NIH): the National Institute of Biomedical Imaging and Bioengineering (Grant No. EB00682, EB-006521), and the National Human Genome Research Institute (Grant No. HG002655).

REFERENCES

1. Wegner GJ, Lee HJ, Corn RM. Characterization and optimization of peptide arrays for the study of epitope-antibody interactions using surface plasmon resonance imaging. *Anal. Chem* 2002;74:5161–5168. [PubMed: 12403566]
2. Jordan CE, Frey BL, Kornguth S, Corn RM. Characterization of Poly-L-lysine adsorption onto alkanethiol-modified gold surfaces with polarization-modulation Fourier transform infrared spectroscopy and surface plasmon resonance measurements. *Langmuir* 1994;10:3642–3648.
3. Frey BL, Jordan CE, Kornguth S, Corn RM. Control of the specific adsorption of proteins onto gold surfaces with poly(L-lysine) monolayers. *Anal. Chem* 1995;67:4452–4457.
4. Natan, MJ.; Lyon, LA. Surface plasmon resonance biosensing with colloidal Au amplification. In: Feldheim, DL.; Foss, CA., editors. *Metal Nanoparticles: Synthesis, Characterization, and Applications*. New York: Marcel Dekker; 2002. p. 183-205.
5. Homola J, Koudela I, Yee SS. Surface plasmon resonance sensors based on diffraction gratings and prism couplers: sensitivity comparison. *Sensors and Actuators B* 1999;54:16–24.
6. Endo T, Kerman K, Nagatani N, Hiepa HM, Kim D, Yonezawa Y, Nakano K, Tamiya E. Multiple label-free detection of antigen-antibody reaction using localized surface plasmon resonance based core-shell structure nanoparticles layer nanochip. *Anal. Chem* 2006;78:6465–6475. [PubMed: 16970322]
7. Lee K, Lee C, Wang W, Wei P. Sensitive biosensor array using surface plasmon resonance on metallic nanoslits. *J. Biomed. Opt* 2007;12 044023.
8. Yu X, Xu D, Cheng Q. Label-free detection methods for protein microarrays. *Proteomics* 2006;6:5493–5503. [PubMed: 16991201]
9. Ramachandran N, Larson DN, Stark PRH, Hainsworth E, LaBaer J. Emerging tools for real-time label-free detection of interactions on functional protein microarrays. *FEBS J* 2005;272:5412–5425. [PubMed: 16262683]
10. Varma MM, Inerowicz HD, Regnier FE, Nolte DD. High-speed label-free detection by spinning-disk micro-interferometry. *Biosensors and Bioelectronics* 2004;19:1371–1376. [PubMed: 15093207]
11. Miyamoto K, Ishibashi K, Hiroi K, Kimura Y. Label-free detection and classification of DNA by surface vibration spectroscopy in conjugation with electrophoresis. *Appl. Phys. Lett* 2005;86 053902.
12. Landry JP, Zhu XD, Gregg JP. Label-free detection of microarrays of biomolecules by oblique-incidence reflectivity difference microscopy. *Opt. Lett* 2004;29:581. [PubMed: 15035477]
13. Mathias PC, Ganesh N, Chan LL, Cunningham BT. Combined enhanced fluorescence and label-free biomolecular detection with a photonic crystal surface. *Applied Optics* 2007;26:2351–2360. [PubMed: 17415405]
14. Lakowicz JR, Ray K, Chowdhury MH, Zhang J, Fu Y, Szmecinski H, Nowaczyk K. Plasmon-controlled fluorescence: A new paradigm in fluorescence spectroscopy. *The Analyst* 2008;133:1308–1346. [PubMed: 18810279]
15. Lakowicz, JR. *Principles of Fluorescence Spectroscopy*. 3rd edition. New York: Kluwer Academic / Plenum Publishers; 2006.

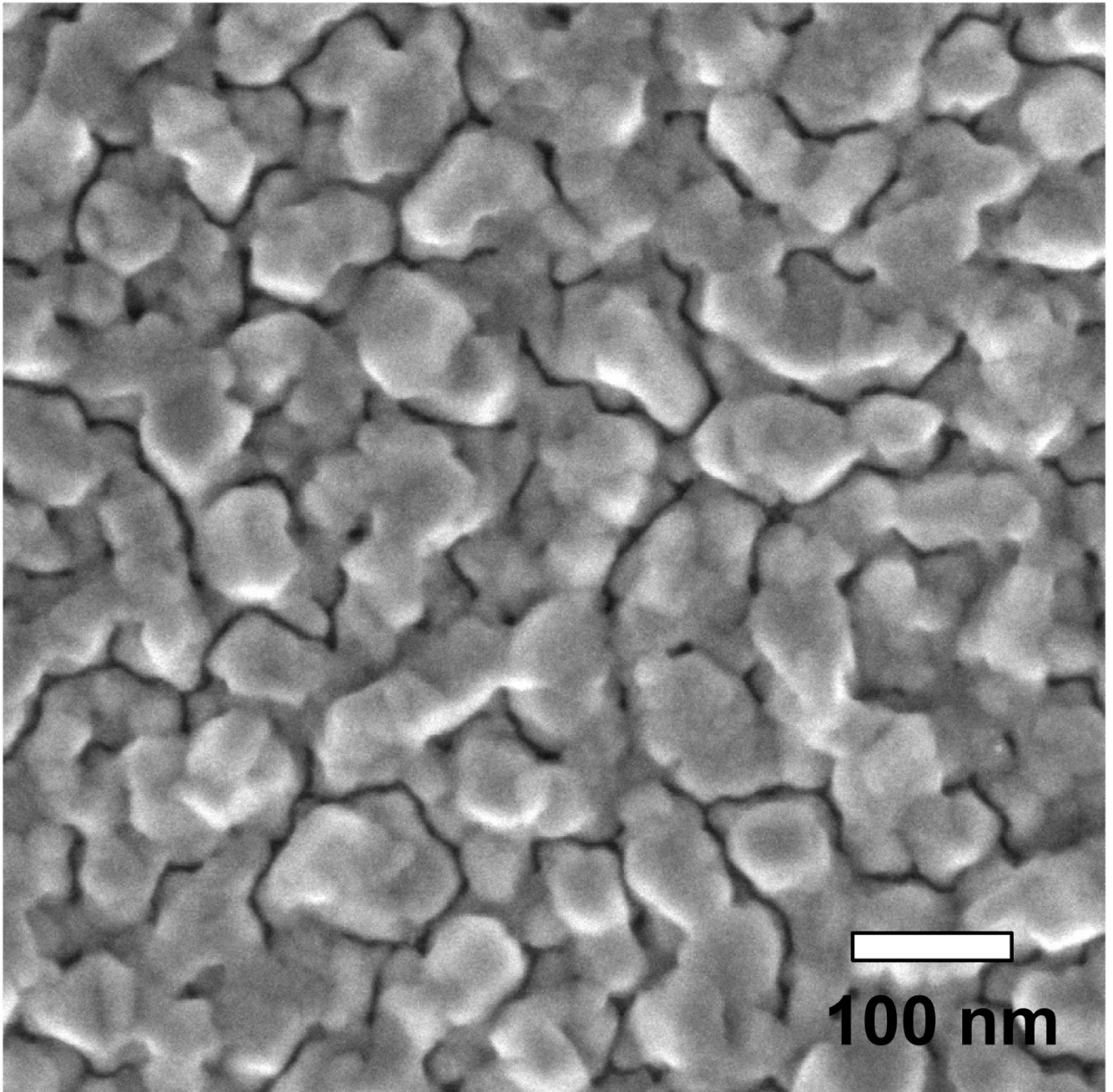


Figure 1.
SEM image of deposited 10nm thick aluminum on quartz substrate.

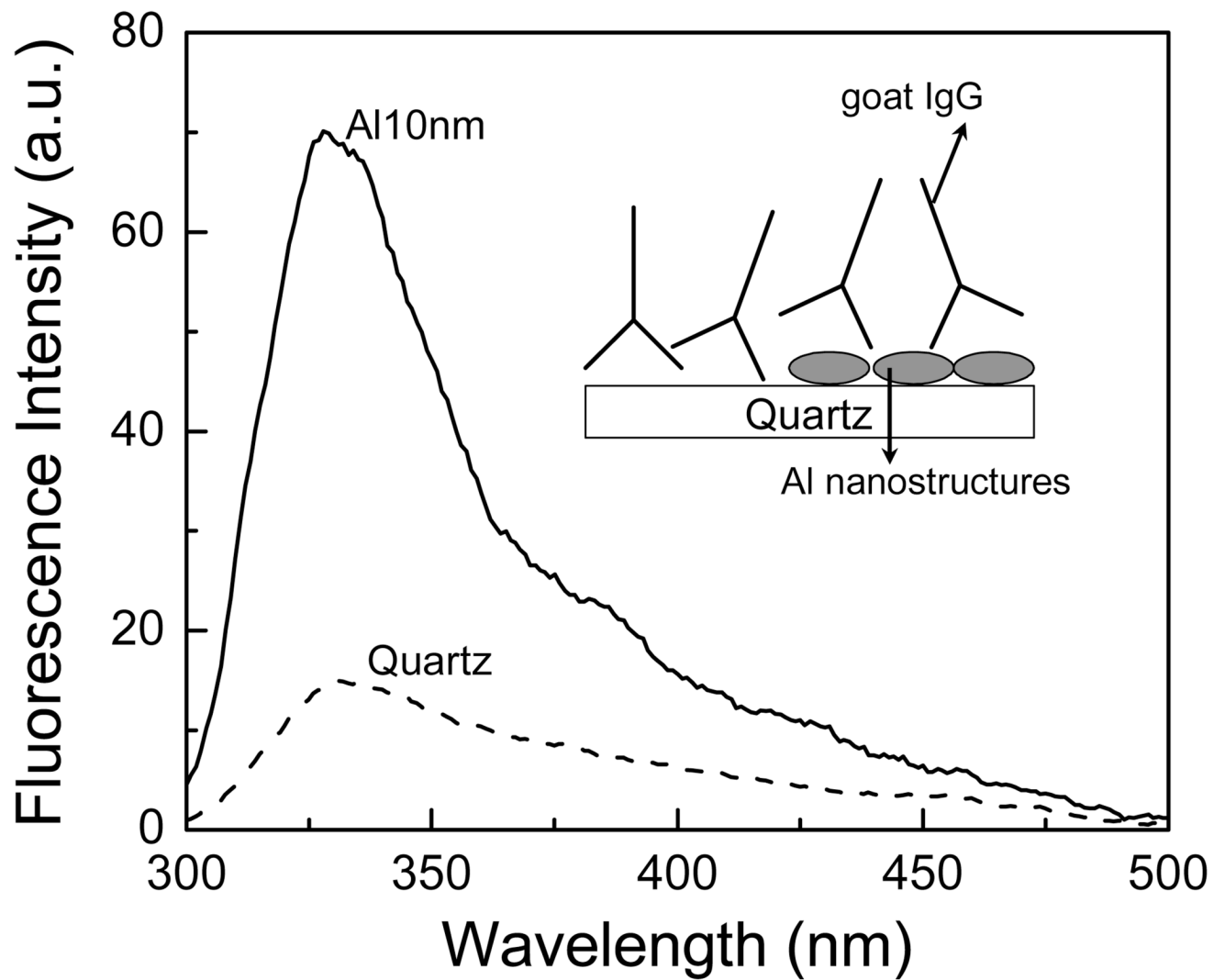


Figure 2.
Emission spectra of goat IgG on quartz and aluminum nanostructured surfaces.

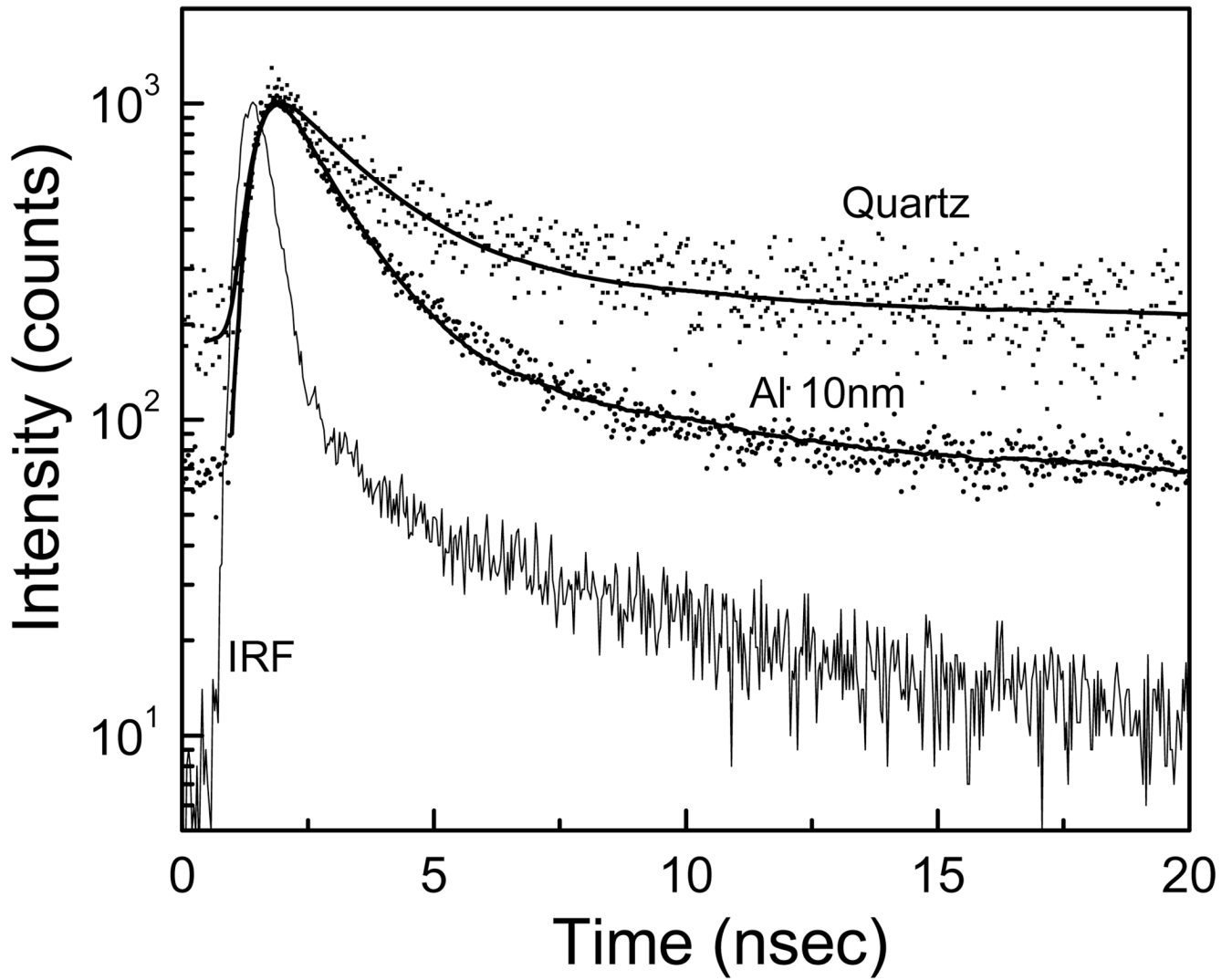


Figure 3.
Intensity decays of IgG on quartz and aluminum nanostructured surfaces.

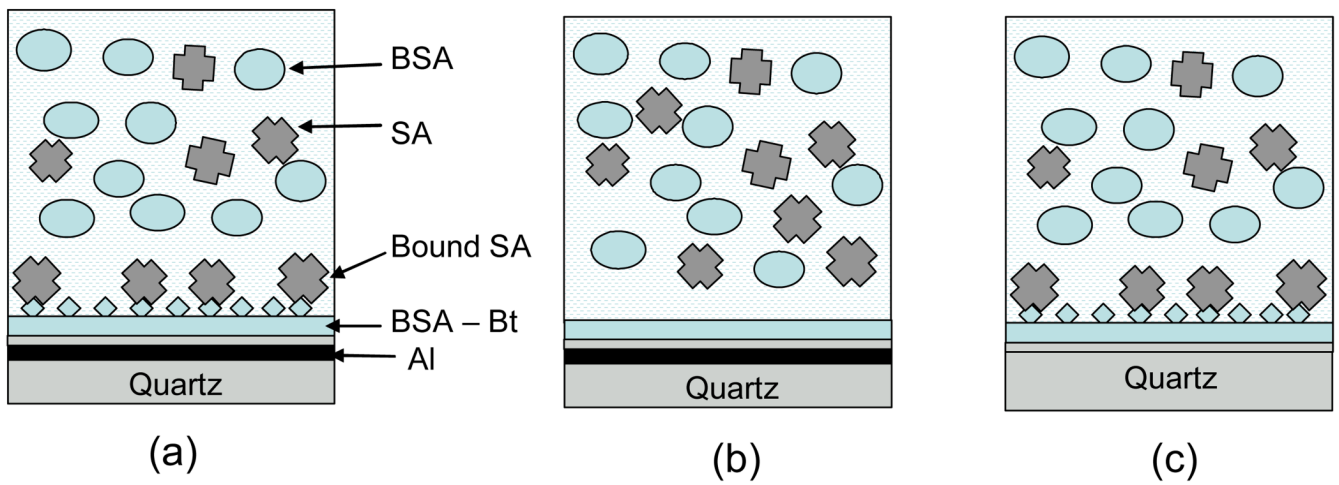


Figure 4. Schematic configurations of MEF-based bioassay for detection of streptavidin (a), control non-binding MEF surface (b) and streptavidin bioassay using non-MEF substrate (d). The sample thickness was 160 μm for reduction of signal from free bulk proteins.

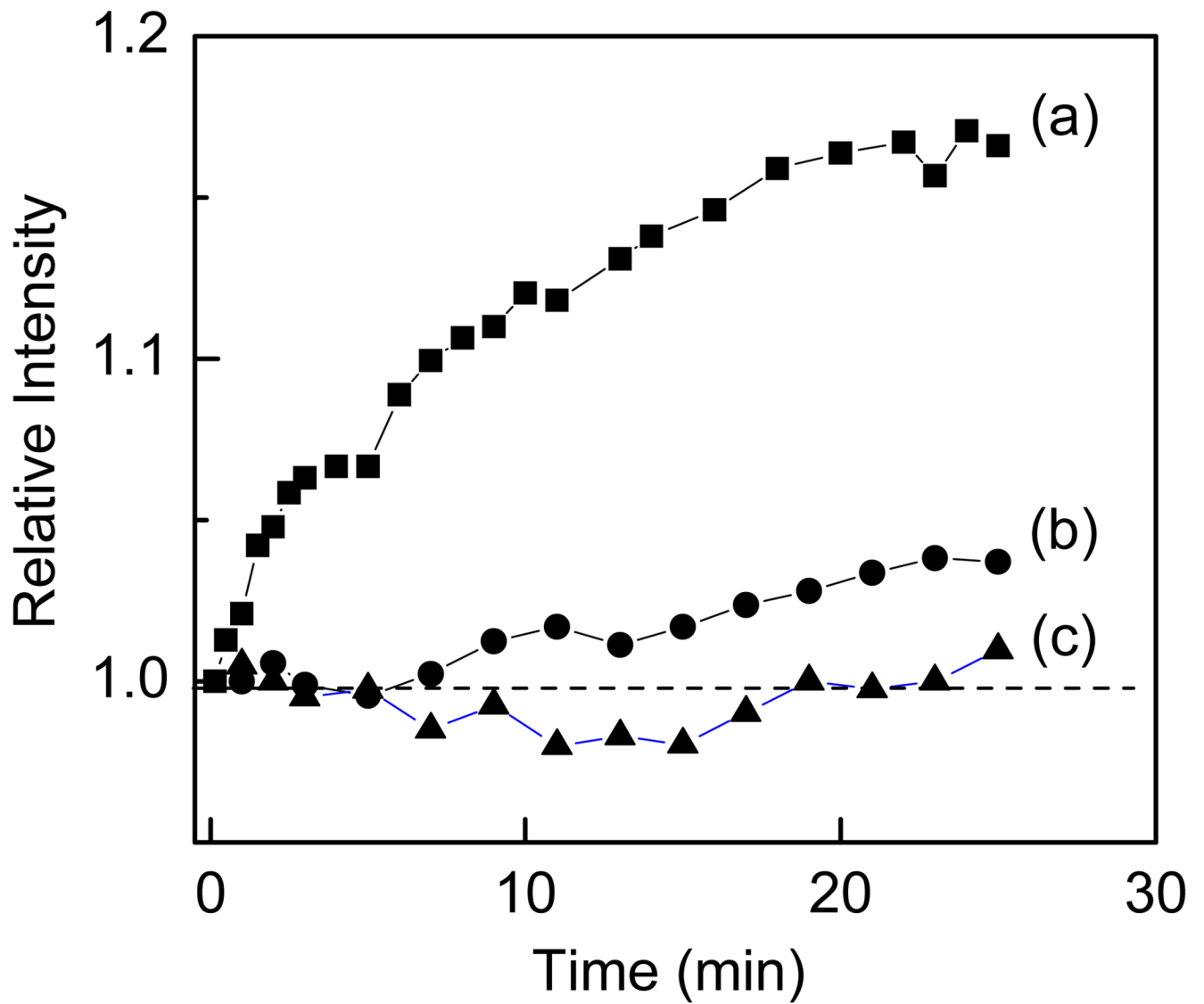


Figure 5. Temporal changes in relative intensity after exposing surfaces (see Figure 4) to the sample containing large concentration of BSA.

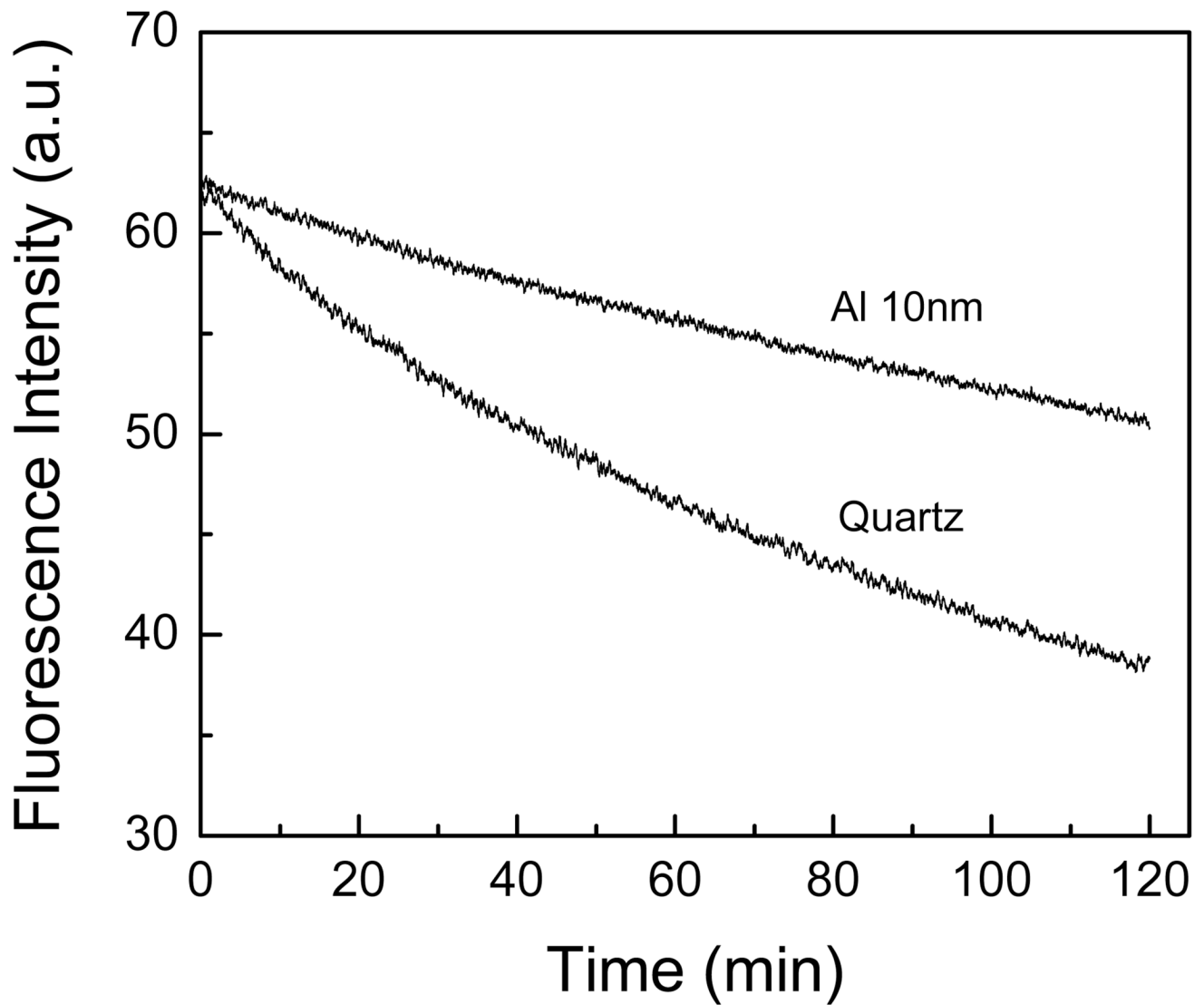


Figure 6. Photostability studies of BSA-biotin-Streptavidin on quartz and aluminum nanostructured surfaces.